Journal of Statistical Physics, Vol. 86, Nos. 5/6, 1997

Stationary Nonequilibrium States in Boundary-Driven Hamiltonian Systems: Shear Flow

N. I. Chernov[1] and J. L. Lebowitz[2]

Received May 13, 1996; final August 15, 1996

We investigate stationary nonequilibrium states of systems of particles moving according to Hamiltonian dynamics with specified potentials. The systems are driven away from equilibrium by Maxwell-demon "reflection rules" at the walls. These deterministic rules conserve energy but not phase space volume, and the resulting global dynamics may or may not be time reversible (or even invertible). Using rules designed to simulate moving walls, we can obtain a stationary shear flow. Assuming that for macroscopic systems this flow satisfies the Navier–Stokes equations, we compare the hydrodynamic entropy production with the average rate of phase-space volume compression. We find that they are equal *when* the velocity distribution of particles incident on the walls is a local Maxwellian. An argument for a general equality of this kind, based on the assumption of local thermodynamic equilibrium, is given. Molecular dynamic simulations of hard disks in a channel produce a steady shear flow with the predicted behavior.

KEY WORDS: Shear flow; deterministic dynamics; Maxwell-demon boundary conditions; entropy production; space-phase volume contraction.

1. INTRODUCTION

Stationary nonequilibrium states (SNS) of macroscopic systems must be maintained by external inputs at their boundaries. Since a complete microscopic description of such inputs is generally not feasible, it is necessary to represent them by some type of modeling. However, unlike systems in equilibrium, which maintain themselves without external inputs and for which one can prove (when not inside a coexistence region of

[1] Department of Mathematics, University of Alabama in Birmingham, Birmingham, Alabama 35294; e-mail: chernov@math.uab.edu.

[2] Department of Mathematics, Rutgers University, New Brunswick, New Jersey 08903; e-mail: lebowitz@math.rutgers.edu.

0022-4715/97/0300-0953$12.50/0

822/86/5-6-4

the phase diagram) that bulk behavior is independent of the nature of the boundary interactions, we do not know how different microscopic modeling of boundary inputs, representing fluxes of matter, momentum, or energy, affects the resulting SNS.

What is observed experimentally is that in regimes close to equilibrium, when the fluxes are small, the bulk macroscopic behavior is determined by the unique solution of the hydrodynamic equations, with specified boundary conditions on the hydrodynamic variables such as density, temperature, and fluid velocity.[1] The situation may change dramatically, however, as soon as the driving foces become sufficiently large for this solution to lose stability. We can then have the formation of coherent structures, such as rolls or hexagons, whose pattern is influenced by details of the boundary conditions.[2]

Even in the absence of hydrodynamic instabilities, e.g., in passive heat conducting systems or fluids in regimes of laminar flow, the SNS generally have *very* long range microscopic correlations, with slow power-law decay, which can be measured experimentally.[3] This raises the possibility that even in regimes of hydrodynamic stability the modeling of the boundary inputs may have global, albeit subtle, effects on the nature of the SNS. In fact it is known that, even in the near-equilibrium regime, different modelings of the external drives produce very different types of microscopic measures of (what appears to be) the same macroscopic SNS. Thus, stochastic drives, such as thermal boundaries in which the particles acquire, following a collision with the walls, a specified Maxwellian velocity distribution, generally lead to stationary measures absolutely continuous with respect to Liouville measure.[4] The same is true for systems driven by collisions with some simple kinds of Hamiltonian infinite-particle reservoirs specified by a given distribution prior to the collisions.[5] Deterministic thermostatting schemes, on the other hand, yield measures singular with respect to Liouville measure.[6-9]

It is quite possible, even likely, that these great differences in the structure of the microscopic SNS (mSNS) do not have any significant effect on the bulk properties of stable macroscopic SNS (MSNS). This is what happens for macroscopic equilibrium systems which can be described by a variety of microscopic ensembles, e.g., the canonical or microcanonical.[10] Unlike equilibrium, however, it is far from clear at present how to characterize essential global features of mSNS. We do expect, however, that *locally* such system will be close to an equilibrium state, at least when the inputs are confined to the boundaries.[11] Indeed, as we shall discuss further later, this property of local thermodynamic equilibrium (LTE) holds the key to understanding SNS of macroscopic systems in the hydrodynamic regime.

Questions regarding the nature of mSNS have recently come to the fore due to the combination of computer and analytical investigations of SNS with various deterministic thermostatting devices.[6-10,12-18] The simulations have shown that the stationary states produced by these drives behave, at least as far as linear transport coefficients and other gross properties of MSNS go, in reasonable accord with known experimental and theoretical results. In addition, the simulations have found unexpected interesting microscopic structures in these singular measures, e.g., pairing rules for the Lyapunov exponents, a formula for large fluctuations in the phase-space volume contraction rate, etc.

The rigorous mathematical analysis of such systems has confirmed some aspects of the simulation results.[9,14] This has led Gallavotti and Cohen[15] (see also refs. 10 and 16) to postulate what they call the "chaotic hypothesis," based on Ruelle's principle for turbulence:

"A many particle system in a stationary state can be regarded, for the purpose of computing macroscopic properties, as a smooth dynamical system with a transitive Axiom A global attractor. In the reversible case it can be regarded, for the same purposes, as a smooth transitive Anosov system."

This hypothesis was shown by Gallavotti and Cohen to imply, for SNS produced by reversible thermostatted dynamics a formula for the fluctuation in the phase-space volume contraction rate in agreement with the computer simulations[13] and to be generally consistent with known results, at least when the driving is not too large[16] (see also refs 17 and 18). It also implies, or even presupposes, a strong form of "equivalence of ensembles" for SNS with specified macroscopic flows. This is, as already noted, certainly in accord with experience on SNS close to equilibrium, where it can be understood as an expression of the existence of LTE. It may, however, also be true more generally, at least in some form.

In the present paper we investigate a new class of models in which the microscopic dynamics in the bulk of the system is Hamiltonian and reflection at the boundaries is deterministic and energy-conserving. This permits us to define a phase-space flow $\dot{X}=\mathscr{F}(X)$, X a point in (a fixed energy surface of) the system's phase space. In this respect our model is similar to the bulk thermostatting schemes mentioned earlier.[6-8] Unlike those schemes, however, which modify the equations of motion in the bulk of the fluid, somthing which is computationally useful but has no counterpart in real physical systems, our model is fully realistic away from the boundaries. In this respect it is similar to models in which the driving force is a "boundary layer" of reservoir particles or is given by stochastic thermal boundaries.[4,5,19] Our combination of realistic bulk dynamics and deterministic

boundary drives offers a simple model of an mSNS which can be investigated by means of classical dynamical systems theory. It will hopefully lead to a better understanding of SNS representing real systems.

Our main conclusion can be summarized as follows: Deterministic boundary-driven models, reversible or not, accurately represent the bulk behavior of MSNS. There is an equality in these models between phase-space volume contraction and hydrodynamic bulk entropy production for SNS of macroscopic systems in LTE. Plausible arguments of why this should be so and of how to connect entropy production in nonequilibrium states generated by different modelings of the inputs are given in Section 8. This is preceded by a detailed description of analytic and computer simulation results for specific models producing shear flow. A preliminary account of this work is presented in ref. 20.

2. DESCRIPTION OF MODELS

To make the analysis as concrete as possible we shall consider here SNS representing shear flow in a two-dimensional system; we imagine this to be the surface of a cylinder of height and perimeter L, or a square box with periodic boundary conditions along the x axis, i.e., we identify the left and right sides at $x = \pm L/2$. On the top and bottom sides of the box, $y = \pm L/2$, are rigid walls at which stand watchful Maxwell demons who make the particles reflect according to rules satisfying the following two conditions: (i) the reflected velocity is determined by the incoming one and is energy-conserving; (ii) the particles at the top wall are driven to the right, and those at the bottom wall are symmetrically driven to the left. The purpose of rule (ii) is to imitate moving walls and thus produce a shear flow in the bulk of the system. The use of a two-dimensional system and of symmetric rules for top and bottom is for simplicity only and the reader is free to imagine instead a three-dimensional channel with different reflection rules at top and bottom.

Since reflections at the wall preserve the particle speed, the reflection rule can be defined in terms of angles. For a particle colliding with the top wall, let φ and $-\psi$ be, respectively, the angles which the incoming and outgoing velocities make with the positive x axis, the direction of the "wall velocity," so that $0 \leqslant \varphi, \psi \leqslant \pi$. At the bottom wall, the angles are measured between the velocity vectors and the negative x axis. Then, any reflection rule is completely specified by a function $\psi = f(\varphi, v)$, where v stands for the speed of the particle.

For simplicity, we only study here functions independent of v, which are the same for both walls, so that

$$\psi = f(\varphi), \qquad 0 \leqslant \varphi, \ \psi \leqslant \pi \tag{2.1}$$

In particular, the identity function $f(\varphi)=\varphi$ corresponds to elastic reflections, and $\psi=\pi-\varphi$ gives complete velocity-reversal reflections.

One particularly simple reflection rules is given by

$$\psi=\begin{cases}\varphi, & \varphi\leqslant\varphi_0\\ \pi-\varphi, & \varphi>\varphi_0\end{cases} \tag{2.2}$$

which, for $\pi/2\leqslant\varphi_0<\pi$, clearly satisfies (ii). Under this rule, particles moving "in the direction of the wall velocity" with $\varphi\leqslant\varphi_0$ reflect elastically at the wall, while those moving "opposite the wall velocity" $\varphi>\varphi_0$ will reflect straight back, with the velocity vector reversed. This rule is noninvertible, and is discussed further in elsewhere[18] (see also ref. 23). Here we shall focus our attention on two invertible rules that we found particularly interesting and which we used in our molecular dynamics simulations. They are

$$\psi=(\pi+b)-[(\pi+b)^2-\varphi(\varphi+2b)]^{1/2} \tag{2.3}$$

with $b\geqslant 0$ and

$$\psi=c\varphi \tag{2.4}$$

with $0<c\leqslant 1$. We call these the b-model and the c-model, respectively.

The graph of the function (2.3) is a circular arc terminating at the points $(0, 0)$ and (π, π) lying below the diagonal $\psi=\varphi$. This function has the symmetry $\varphi=f^{-1}(\psi)=\pi-f(\pi-\psi)$, which makes the dynamics time-reversible. Time-reversal symmetry, which is present in Hamiltonian dynamics as well as in the usual Gaussian thermostatted models,[6,9] means that the system retraces its trajectory backward in time following a velocity reversal of all the particles. This symmetry plays an essential role in some of the analysis in ref. 15. The c-model is not time-reversible. Similarities and differences between the b- and c-models are therefore of particular interest in determining the range of universality present in SNS. We shall in fact see that the b- and c-models behave in a similar way.

3. THE STATIONARY STATE

Let us consider now the time evolution and the nature of the stationary states we might expect with our b- or c-dynamics for a system of N particles with total energy E, and average particle and energy densities $\bar{n}=N/L^2$ and $\bar{e}=E/L^2$, respectively. For the sake of concreteness imagine the particles to be hard disks with unit mass and unit diameter, so E is

just their kinetic energy. When $b = \infty$ or $c = 1$ the boundary conditions correspond to elastic reflections and so, for N greater than one, but less than some jamming value, we expect that, starting with any initial measure absolutely continuous with respect to the Liouville measure on the $H = E$ surface, the ensemble density will approach (weakly), as $t \to \infty$, the uniform density on this surface, i.e., we expect the microcanonical ensemble of a system of hard disks with mixed periodic and reflecting boundaries to be ergodic and mixing. (There is actually, in addition to the energy, also a conserved total x momentum, which we fix to zero and ignore.)

When $b \neq \infty$ or $c \neq 1$ the rules will clearly produce a drift to the right near the top wall and to the left near the bottom wall. This drift should produce, for L large compared to the man free path $(\pi\bar{n})^{-1}$, an mSNS representing a system with a shear flow.[19,20] On the microscopic level we expect now that any initial ensemble density absolutely continuous with respect to the microcanonical ensemble will evolve, as $t \to \infty$, to a stationary measure $\hat{\mu}$ whose Hausdorff dimension[3] is less than the dimension of the energy surface.[6,10] Such behavior is proven for a single particle subjected to an external force moving among a fixed periodic array of scatters.[9]

We note that when both walls "move" in the *same* direction, the x component of the total momentum of the system is a monotone-nondecreasing function of the number of collisions with the walls. Since this is bounded above, the initial ensemble density must converge (at least in some weak sense) to a measure whose support is on configurations in which the particles all move parallel to the x axis. This situation is rather pathological. We expect our system with top and bottom walls moving in opposite directions to reach and stay in an LTE state at least when the shear is not too large. This is consistent with $\hat{\mu}$ being singular: even with its Hausdorff dimension being only a fraction of the dimension of the energy surface.[10]

Assuming that our system will indeed go, for N large, $\bar{n}$ and e fixed, to an MSNS representing a fluid in shear flow, as is indeed seen in our computer simulations to be described later, we consider now briefly the purely hydrodynamic description of such an MSNS. This is given by the stationary solution of the compressible Navier–Stokes equations for the fluid velocity in the x direction $u(y)$, the temperature $T(y)$, and density $n(y)$ in a uniform channel of width L in which top and bottom walls move

[3] Here the Hausdorff dimension of the measure $\hat{\mu}$ is, in accord with Young[21] and Pesin,[22] the minimum of the Hausdorff dimension of subsets of full measure. (Other definitions of Hausdorff dimensions of measures are sometimes used, which makes this notion confusing.) The Hausdorff dimension in the Young–Pesin version coincides with the information dimension for systems with nonvanishing Lyapunov exponents.[22] Note that the support of the measure $\hat{\mu}$ may or may not be the entire phase space.

with velocities $\pm u_b$ in the x direction, have the same temperature T_b, and we impose a no-slip boundary condition.[1]

These equations, which are derived on the assumption of LTE,[11] have the form[1,6]

$$\frac{d}{dy} p(n, T) = 0$$

$$\frac{d}{dy}\left(\eta \frac{du}{dy}\right) = 0 \tag{3.1}$$

$$\frac{d}{dy}\left(\kappa \frac{dT}{dy}\right) + \eta \left(\frac{du}{dy}\right)^2 = 0$$

Here $p(n, T)$ is the (local) equilibrium pressure of the system at constant density $n(y)$ and temperature $T(y)$, $\eta(n, T)$ is the viscosity, and $\kappa(n, T)$ is the heat conductivity. Equations (3.1) are to be solved subject to the boundary conditions $u(\pm L/2) = \pm u_b$, $T(\pm L/2) = T_b$ and fixed average particle density $L^{-1} \int_{-L/2}^{L/2} n(y)\, dy = \bar{n}$. This gives

$$p(n, T) = p(n_0, T_0), \qquad du/dy = \Pi/\eta, \qquad -\kappa\, dT/dy = J(y) = \Pi u(y) \tag{3.2}$$

where $n_0 = n(0)$, $T_0 = T(0)$, Π is the *constant* x-momentum flux in the negative y direction, $J(y)$ is the heat flux in the positive y direction, and we have used the symmetry of the flow about $y = 0$. These equations can be solved once p, κ, and η are given as functions of n and T. The solution will be unique when the average shear $\gamma = 2u_b/L$ is small.[24]

Equation (3.2) can be integrated further to give

$$u(y) = \Pi y \left[\frac{1}{y} \int_0^y \frac{1}{\eta}\, dy\right], \qquad \frac{dT}{dy} = -\frac{1}{2}\left(\frac{\eta}{\kappa}\right) \frac{d}{dy} u^2 \tag{3.3}$$

so that

$$\Pi = \bar{\eta}\gamma, \qquad \frac{1}{\bar{\eta}} = \frac{1}{L} \int_0^L \frac{dy}{\eta(n, T)} \tag{3.4}$$

For dilute gases, η/κ is a constant independent of n and T, in which case

$$T(y) = T_0 - \frac{1}{2}\left(\frac{\eta}{\kappa}\right) u^2(y) \tag{3.5}$$

In some cases the y variation in η and κ are so small across the channel that we have an essentially linear flow regime with

$$u(y) = \gamma y, \qquad T(y) = T_0 - (\eta/2\kappa)\,\gamma^2 y^2, \qquad \Pi = \eta\gamma \tag{3.6}$$

The constancy of p together with the specified average density then determines $n(y)$.

4. ENTROPY PRODUCTION IN SNS

Entropy plays a central role in determining the time evolution and (final) equilibrium states of isolated macroscopic systems. Its microscopic interpretation as the log of the phase-space volume of all microstates consistent with a specified macroscopic description was well understood by Boltzmann and the other "founding fathers" of statistical mechanics, although there is still much fuzziness and outright confusion surrounding the subject. We refer the reader to ref. 25 and references there for a discussion.

The role of entropy and/or entropy production in SNS is also very important, although much less clear. By their nature truly SNS cannot occur in an isolated finite system evolving under Hamiltonian (or quantum) dynamics—the only truly stationary macroscopic state for such a system being the equilibrium one. The situation can be different for *ab initio* infinite systems,[26] but we shall not discuss that here. We shall instead describe now various aspects of entropy production in the simple SNS corresponding to stable shear flow in the finite systems considered here. We will then discuss in Section 8 the connection between them, and what they teach us.

4.1. Hydrodynamics

The *hydrodynamic* entropy production σ per unit volume in our stationary system is given by the Onsager form[17] (see in particular Chapter 14 in ref. 1 and Section 2.2 in ref. 7)

$$\sigma(y) = \frac{\Pi}{T}\frac{du}{dy} + J(y)\frac{d}{dy}\left(\frac{1}{T}\right) = \Pi\frac{d}{dy}\left(\frac{u}{T}\right) \tag{4.1}$$

where we used (3.2) in the second equality. The total hydrodynamic entropy production $\bar{R}$ due to the dissipative fluxes in the steady state in then

$$\begin{aligned}\bar{R} &= \int_{\text{Volume}} \sigma\, d\mathbf{r} = \int_{\text{Surface}} [\Pi u/T]\, ds = \int_{\text{Surface}} \bar{J}_h/T\, ds \\ &= \bar{J}_h/T_h = 2L^2\Pi(u_h/L)/T_h = L^2\Pi\gamma/T_h\end{aligned} \tag{4.2}$$

where $\bar{j}_h$ is the heat flux per unit length and $\bar{J}_h$ the total flux to the walls and we have taken the channel to be of length L with periodic boundary conditions in the x direction.

Equation (4.2) is interpreted in the macroscopic formulation of irreversible thermodynamics[1] as an equality, in the stationary state, between the hydrodynamic entropy produced in the interior and the entropy carried by the entropy flux, equal to J_h/T_h, to the walls of the container. To maintain such a steady state in an experimental situation requires external forces acting on the walls to make them move with velocities $\pm u_h$. The work done by these forces, $|\Pi u_h|$ per unit wall area, is converted to heat in the bulk of the fluid by the viscosity and then absorbed by the walls acting as infinite thermal reservoirs. The steady-state hydrodynamic entropy production in the system $\bar{R}$ is also carried to the walls by this heat flux. If we imagine the wall as "equilibrium" thermal bath at temperature T_h, then $\bar{R}$ is equal to the rate of their entropy increase ($dS_{eq} = dU/T$): note that we are assuming here that there is no slip between the temperature of the fluid at the walls and the temperature of the walls.

4.2. Microscopic: Stochastic Reservoirs

The existence of macroscopic steady states satisfying the compressible Navier–Stokes equations (3.1) can be proven in suitable scaling limits by starting from the Boltzmann equation.[24] In such analysis the wall are typically modeled by stochastic thermal boundaries; following collisions with the wall, particles have a Maxwellian velocity distribution with mean $\pm u_h$ and temperature T_h. Going beyond the mesoscopic description given by the Boltzmann equation, it is expected that such thermal boundaries will produce similar SNS for general fluid systems, which will be described, on the microscopic level, by a stationary measure on the phase space having a density $\bar{\mu}$ absolutely continuous with respect to Liouville measure.[5] In fact it is possible to show, for systems in contact with a thermal reservoir at temperature T, that the total "ensemble entropy production"

$$\mathscr{R}(t) = \dot{S}_G(t) + \langle \tilde{J} \rangle / T \tag{4.3}$$

is nonnegative.[5] Here

$$S_G(t) \equiv S_G(\mu(X, t)) \equiv -\int \mu(X, t) \log \mu(X, t)\, dX \tag{4.4}$$

is the system's Gibbs entropy, dX is the Liouville volume element in the phase space, and $\langle \tilde{J} \rangle$ is the ensemble average of a phase-space function

$\tilde{J}(X)$ representing energy flux to the reservoir. At the same time the rate of change of the man energy in the system is given by

$$\frac{d}{dt}\int \mu H\, dx = \langle \dot{H} \rangle = -\langle \tilde{J} \rangle + \langle \tilde{W} \rangle \tag{4.5}$$

where $\langle \tilde{W} \rangle$ is the average mechanical work done on the system by some external force, e.g., one produced by moving *rough* walls to the system in a channel.[19]

In the stationary state obtained in the limit $t \to \infty$, $\mu = \bar{\mu}$, so $\langle H \rangle$ and S_G are constant with $\langle W \rangle = \langle \tilde{J} \rangle$ and $\mathscr{R} = \bar{\mathscr{R}} = \langle \tilde{J} \rangle / T = \langle W \rangle / T$. Hence if we identify $\langle \tilde{J} \rangle$ with J_h, then $\bar{\mathscr{R}}$ is equal to $\bar{R}$ given in (4.2). For a system in contact with only a thermal reservoir, the stationary state is the equilibrium one and $\mathscr{R}(t) = d/dt\,[S_G - \langle H \rangle / T] \to 0$ as $t \to \infty$ (see ref. 27 and Section 8).

4.3. Microscopic: Deterministically Driven Systems

Let us turn now to our models, where the flow is deterministic and collisions with the boundaries conserve energy. It is not clear at all *a priori* what should now correspond at the microscopic level to the hydrodynamic entropy production in our system. Following the work in refs. 7–9, we note that for a deterministic flow in the phase space the rate of change of the systems Gibbs entropy defined in (4.4) is given by

$$\dot{S}_G(t) = \int \mu(X, t)(\operatorname{div} \dot{X})\, dX = -M(t) \tag{4.6}$$

This vanishes for an isolated system evolving according to Hamiltonian dynamics for which $\operatorname{div} \dot{X} = 0$, but not for dynamics which does not conserve Liouville volume. Furthermore, since we expect the stationary measure for our dynamics $\hat{\mu}$ to be singular with respect to Liouville measure, we will have $S_G(t) \to_{t \to \infty} -\infty$. At the same time since the convergence of μ to $\hat{\mu}$ is in the weak sense, we might have a nonvanishing limit

$$\dot{S}_G(t) \to \int \hat{\mu}(X)(\operatorname{div} \dot{X})\, dX = -\bar{M} \tag{4.7}$$

We can then interpret $\bar{M}$, the average compression rate of phase-space volume per unit time, as the "measure entropy production" in the stationary state. The existence and negative of the limit in (4.7) was proven in ref. 9 for a simple bulk thermostatted model. The nonnegativity of $\bar{M}$ for a stationary $\hat{\mu}$ is proven in a suitable general setting by Ruelle.[23]

The behavior of $\dot{S}_G(t)$ in the driven deterministic case is to be constrasted with the case of stochastic reservoirs consider earlier, where the stationary masure has a smooth density with $\dot{S}_G(t) \to 0$ as $t \to \infty$, while $\mathscr{R}(t) \to \bar{\mathscr{R}} = \bar{R}$, the positive hydrodynamic entropy production in the MSNS. Now in the bulk thermostatted models,[7 9] the equations of motions are such that $\bar{M}$ is automatically equal to the ensemble average of microscopic quantities, which can be identified with thermodynamic forces and fluxes such as appear in the macroscopic entropy production. This is not the case for the models considered here. We have no *a priori* prescription of u or T anywhere in the system and phase-space volume gets compressed only at collisions of a particle with the wall, the bulk dynamics being Hamiltonian. We therefore need to investigate here the relationship, if any, between $\bar{M}$ and $\bar{R}$ for our system. Unfortunately, a direct computation, using only the given dynamics, is totally out of reach of our present mathematical abilities. What we shall do instead in the next section is to make some reasonable assumptions on the nature of the microscopic SNS in the limit when our system becomes of macroscopic size. It will turn out that these assumptions, which are satisfied for a system in LTE, lead to an equality between $\bar{M}$ and $\bar{R}$. This will be checked and confirmed by computer simulations in Section 7. We will then argue in Section 8 that such an equality holds in general when the macroscopic system is in a state of LTE.

Remark. It might be feasible to carry out such a rigorous analysis of our model within the context of the Boltzmann equation, in analogy to what is done for stochastic walls in ref. 24. Numerical simulations on models b and c using the direct simulation Monte Carlo method for simulating the Boltzmann collision term inside the channel are now being carried out.[26] The results appear consistent with those in Section 7.

5. CALCULATION OF *M* IN THE HYDRODYNAMIC REGIME

To obtain the rate of compression $\bar{M}$ for our system, we observe that our dynamics preserves phase-space volume except at collisions of a particle with a wall. Since these collisions take place "instantaneously," we can compute the compression occurring at a single collision—ignoring the rest of the particles. The compression is then just equal to the ratio of the "outgoing" one-particle phase-space volume $(dx'\, dy'\, dv'_x\, dv'_y)$ to the incoming one $(dx\, dy\, dv_x\, dv_y)$ in a time interval dt containing the collision. A little thought show that $dx' = dx$ and

$$|dv'_x\, dv'_y / dv_x\, dv_y| = |v'\, dv'\, d\psi| / (v\, dv\, d\phi| = |d\psi / d\phi|$$

where ϕ and ψ are the incoming and outgoing angles, related by $\psi = f(\phi)$. Similarly, $|dy'/dy| = |v'_y\, dt/v_y\, dt| = |\sin\psi/\sin\phi|$. Hence in every collision between a particle and the wall the phase-space volume is changed by a factor

$$\left|\frac{\sin\psi\, d\psi}{\sin\varphi\, d\varphi}\right| = \frac{\sin f(\varphi)}{\sin\varphi}\,|f'(\varphi)| = \left|\frac{d\cos f(\varphi)}{d\cos\varphi}\right| \tag{5.1}$$

where f defines the reflection rule (2.1). The phase-space volume will be reduced or increased depending on whether (5.1) is smaller or larger than unity.

The mean exponential rate of compression of the phase-space volume per unit time is then given by

$$\bar{M} = -2\langle N_c \log[f'(\varphi)\sin f(\varphi)/\sin\varphi\rangle_{\hat{\mu}} \tag{5.2}$$

where $N_c(\varphi)$ is the flux of particles entering a collision with the top wall at angle φ. The factor 2 comes from summing over top and bottom walls and the average is taken with respect to the stationary measure $\hat{\mu}$.

An exact evaluation of $\bar{M}$ given in (5.2) is currently far beyond our abilities. To proceed further, we assume now that in the hydrodynamic regime corresponding to $L \gg l$ and $\gamma l \ll 1$, where $l \sim (\pi\bar{n})^{-1}$ is the mean free path between particle–particle collisions, the density $\rho(v_1, v_2)$ of the velocity vectors $\mathbf{v} = (v_1, v_2)$ of particles entering a collision with the walls is Maxwellian with the (to be determined) mean value $(\bar{v}, 0)$ and temperature T_w for the top wall $[(-\bar{v}, 0)$ and T_w for the bottom wall]. That is,

$$\rho(v_1, v_2) = (2\pi T_w^3)^{-1/2}\, v_2 \exp\left(-\frac{(v_1-\bar{v})^2 + v_2^2}{2T_w}\right), \qquad v_2 > 0 \tag{5.3}$$

It will be convenient to rewrite the density (5.3) in polar coordinates, $v_1 = r\cos\theta$ and $v_2 = r\sin\theta$,

$$\rho(r,\theta) = \frac{1}{\sqrt{2\pi}\, T_w^{3/2}}\, r^2 \sin\theta \exp\left(-\frac{\bar{v}^2 + r^2 - 2\bar{v}r\cos\theta}{2T_w}\right), \qquad 0 \leqslant \theta \leqslant \pi \tag{5.4}$$

and denote by $\langle F\rangle$ the average of any function $F(r,\theta)$ with respect to (5.4).

The average momentum transfer "from wall to wall" $\hat{\Pi}$ is now given by

$$\hat{\Pi} = n_c\langle \Delta v_1\rangle = n_c\langle v_{1,\mathrm{out}} - v_{1,\mathrm{in}}\rangle \tag{5.5}$$

where n_c is the "collision rate," i.e., the average number of collisions with the top wall per unit time per unit length, which will have to be computed later. In our polar coordinates (r, θ) this value is

$$\begin{aligned}\hat{\Pi} &= n_c \langle r(\cos f(\theta) - \cos\theta)\rangle \\ &= \frac{n_c}{\sqrt{2\pi}\, T_w^{3/2}} \int_0^\infty \int_0^\pi [\cos f(\theta) - \cos\theta]\, r^3 \sin\theta \\ &\quad \times \exp\left(-\frac{\bar{v}^2 + r^2 - 2\bar{v}r\cos\theta)}{2T_w}\right) d\theta\, dr \end{aligned} \tag{5.6}$$

In order to keep the "velocity" of our walls from growing with L when L becomes macroscopic, which would certainly take the system away from local equilibrium, we need to consider situations in which $\hat{\Pi}$, like the hydrodynamic Π in Section 3, is of order $(1/L)$. This requires that the reflection rules (2.1) be close to the identity, i.e., we put

$$\psi = f(\varphi) = \varphi + \delta f_1(\varphi) + \delta^2 f_2(\varphi) + o(\delta^2) \tag{5.7}$$

with f_1, f_2 some fixed functions on $[0, \pi]$. In fact, as seen from (5.6), δ has to be $O(L^{-1})$. For our b-model (2.3) we can set $\delta = 1/b$, and then (5.7) will have the form

$$\psi = \varphi - \delta\varphi(\pi - \varphi) + \delta^2\varphi(\pi - \varphi)^2 + o(\delta^2) \tag{5.8}$$

For our c-model (2.4) we can set $\delta = 1 - c$, and so

$$\psi = \varphi - \delta\varphi \tag{5.9}$$

(Our calculations, however, are not restricted to these two models.)

Expanding $\hat{\Pi}$ in δ gives

$$\begin{aligned}\hat{\Pi} &= n_c \langle r[-\sin\theta\, \delta f_1(\theta) + O(\delta^2)]\rangle \\ &= -\frac{n_c \delta}{\sqrt{2\pi}\, T_w^{3/2}} \int_0^\infty \int_0^\pi f_1(\theta)\, r^3 \sin^2\theta \exp\left(-\frac{\bar{v}^2 + r^2 - 2\bar{v}r\cos\theta)}{2T_w}\right) d\theta\, dr \\ &\quad + O(\delta^2) \end{aligned} \tag{5.10}$$

The last double integral depends on the so-far-inknown parameters $\bar{v}$ and T_w, and we denote it by $I(\bar{v}, T_w)$.

We next assume that the steady state will indeed correspond to a shear flow described (on the average) by the hydrodynamic equations in Section 3, and identify the $\hat{\Pi}$ with Π and T_w with T_b there. Since, however,

we are not given T_b and u_b, they have to be determined from the given data, assuming the system to be in LTE. Thus the determination of T_w is now done on the basis that the system has a fixed energy E so that

$$\frac{1}{L}\int_0^L n(y)\left[T(y)+\frac{1}{2}u^2(y)\right]dy=\frac{E}{L^2}=\bar{e} \tag{5.11a}$$

while the man horizontal velocity of the particles near the wall can be taken as the man between ingoing and outgoing velocities,

$$u_b=\langle v_{1,\text{out}}+v_{1,\text{in}}\rangle/2=\bar{v}+O(\delta) \tag{5.11b}$$

The solution of (3.1) which determines $u(y)$, $T(y)$, and $n(y)$ in terms of u_b T_b, and $\bar{n}$ will now be determined entrirely by the *a priori* given $\bar{e}$, $\bar{n}$ and the rule $f(\varphi)$, via (5.10) and (5.11). The computation becomes straightfoward in the linear approximation (3.6); see Eqs. (6.6)–(6.9) in the next section.

We study now the case $\delta\to 0$ and $L=a/\delta$ with some fixed $a>0$. Then, the wall velocity u_b is proportional to ΠL and thus does not vanish as $\delta\to 0$. Using (4.2) and (5.10), we find that the hydrodynamic entropy production $\bar{R}$ in this limit is given by

$$\bar{R}=-\frac{2an_c\bar{v}}{\sqrt{2\pi}\,T_w^{5/2}}I(\bar{v},T_w)+o(1) \tag{5.12}$$

To obtain the compression rate $\bar{M}$ in this limit we expand (5.2) in δ using our ansatz (5.3). This gives, upon replacing N_c by $2n_cL$,

$$\begin{aligned}\bar{M}/(2n_cL)&=-\langle\log[f'(\varphi)\sin f(\varphi)/\sin\varphi)\rangle\\&=-\langle f_1(\varphi)\cos\varphi/\sin\varphi\rangle\,\delta-\langle f_1'(\varphi)\rangle\,\delta+o(\delta)\end{aligned} \tag{5.13}$$

Now, integration by parts yields

$$\langle f_1'(\varphi)\rangle=-\int_0^\infty\int_0^\pi f_1(\theta)\,\rho_\theta(r,\theta)\,d\theta\,dr$$

where ρ_θ stands for the partial derivative of the density (5.4) with respect to θ:

$$\rho_\theta(r,\theta)=\frac{\cos\theta}{\sin\theta}\rho(r,\theta)-\frac{\bar{v}r\sin\theta}{T_w}\rho(r,\theta) \tag{5.14}$$

Combining (5.13) and (5.14) then gives

$$\bar{M} = -2\delta L n_c \bar{v} T_w^{-1} \langle f_1(\varphi)\, r \sin\varphi \rangle + o(L\delta)$$
$$= -\frac{2an_c\bar{v}}{\sqrt{2\pi\, T_w^{5/2}}} I(\bar{v}, T_w) + o(1) \tag{5.15}$$

A shorter way to get (5.15) is to rewrite the middle in (5.13) as

$$\left\langle \log\left(1 + \frac{d[\cos f(\varphi) - \cos\varphi]}{d\cos\varphi}\right)\right\rangle = -\delta \left\langle (\sin\varphi)\frac{df_1}{d\cos\varphi}\right\rangle + o(\delta) \tag{5.16}$$

and then do an integration by parts using $\cos\theta$ as a variable. The leading term in (5.16) will be recognized as corresponding to (4.6) for the continuous time action of the thermostats; see the Appendix.

The leading term in the expansion of $\bar{M}$ is thus exactly the same as in that of $\bar{R}$, hence $\bar{M}$ and $\bar{R}$ become equal in the hydrodynamic limit, $L \to \infty$. The essential requirement for the equality is the validity of (5.14). [This is weaker than (5.3), permitting multiplication of the Maxwellian there by an arbitrary function of r, but we do not know of any physically reasonable non-Maxwellian ρ which would satisfy (5.14).] The equality between $\bar{R}$ and $\bar{M}$ in the hydrodynamic regime is thus a nontrivial consequence of our (local equilibrium) assumption (5.3). As already noted, this is an importan difference between our models and the bulk thermostatted models of refs. 7–9. The relation between phase-space volume compression and what *looks like* entropy production is so built into the structure of the dynamics of the latter that there equality holds, essentially by definition, even for systems consisting of just one or a few particles which are certainly not in local equilibrium. This is not the case here. The equality fails for systems with too few particles to be well described by hydrodynamics, as is seen in the next section.

6. SMALL-δ REGIME

Before presenting our numerical simulations, which were obviously done at finite (and not so large) L, we consider the consequences which can be drawn from our assumption (5.3) when $\delta \to 0$ and L is (relatively) large but held fixed. Now the generated shear flow in our system will only be approximately described by the hydrodynamic equation (3.1). Furthermore, u_w as well as $\bar{R}$ and $\bar{M}$ vanish as $\delta \to 0$. Interestingly enough, there is now a difference between the b- and c-models with $\bar{M}/\bar{R}$ remaining finite for the b-model as $\delta \to 0$ (close to unity for moderately large L), while

becoming infinite for the c-model. As we shall see, however, this is connected with the details of the c-model, rather than with its lack of time reversibility.

To compute $\bar{R}$ and $\bar{M}$ in this case it will be necessary to expand various quantities up to second order in δ. Thus,

$$\begin{aligned}\bar{M}/(2n_c L) &= \langle \log[f'(\varphi) \sin f(\varphi)/\sin \varphi] \rangle \\ &= \langle f_1(\varphi) \cos \varphi/\sin \varphi \rangle \, \delta + \langle f_1'(\varphi) \rangle \, \delta \\ &\quad + \langle f_2(\varphi) \cos \varphi/\sin \varphi \rangle \, \delta^2 + \langle f_2'(\varphi) \rangle \, \delta^2 \\ &\quad - \tfrac{1}{2} \langle [f_1'(\varphi)]^2 \rangle \, \delta^2 - \tfrac{1}{2} \langle f_1^2(\varphi)/\sin^2 \varphi \rangle \, \delta^2 + o(\delta^2) \end{aligned} \tag{6.1}$$

This expansion is of course meaningful only if the coefficients of δ and δ^2 are finite, which requires that $f_1(0) = f_1(\pi) = 0$ and that f_1 has finite derivatives at both 0 and π. Our b-model satisfies these assumptions because $f_1(\varphi) = -\varphi(\pi - \varphi)$; see (5.8). The computation of $\bar{M}$ for the c-model, which does not satisfy $f_1(\pi) = 0$, will be done separately.

In order to compute the coefficients in the expansion (6.1), we need to expand the density (5.4), which, using (3.2) or (3.6), depends on δ through the quantities $\bar{v} = O(\delta)$ and $T_w = 1/2 + O(\delta^2)$ to first order in δ. This gives

$$\rho(r, \theta) = 2\pi^{-1/2} r^2 e^{-r^2} \sin \theta + 4\pi^{-1/2} \bar{v} r^3 e^{-r^2} \sin \theta \cos \theta + o(\delta) \tag{6.2}$$

$$\bar{M} = (C_1 + C_2) \, \bar{v}^2 + o(\delta^2) \tag{6.3}$$

with

$$C_1 = 8\eta \left(1 - \frac{\eta}{n_c L}\right)^{-2} \tag{6.4}$$

$$\begin{aligned} C_2 = \frac{2\pi\eta^2}{n_c L} \left(1 - \frac{\eta}{n_c L}\right)^{-1} \left(\int_0^\pi f_1(\theta) \sin^2 \theta \, d\theta\right)^{-2} \\ \times \int_0^\pi \{f_1^2(\theta) \sin^{-1} \theta + [f_1'(\theta)]^2 \sin \theta\} \, d\theta \end{aligned} \tag{6.5}$$

We assume now that for small δ and moderate L, of the kind used in our simulation, the system is reasonably well described by a linear shear flow, Eq. (3.6). We can then find the relation between $\bar{v}$ and δ,

$$\bar{v} = -\frac{L n_c \delta}{2\eta \sqrt{\pi}} \left(1 - \frac{\eta}{n_c L}\right) \int_0^\pi f_1(\theta) \sin^2 \theta \, d\theta + O(\delta^2) \tag{6.6}$$

Similarly we get

$$\Pi = -\frac{2n_c\delta}{\sqrt{\pi}} \int_0^\infty \int_0^\pi f_1(\theta)\, r^3 \sin^2\theta\, e^{-r^2}\, d\theta\, dr + O(\delta^2)$$

$$= -\frac{n_c\delta}{\sqrt{\pi}} \int_0^\pi f_1(\theta) \sin^2\theta\, d\theta + O(\delta^2) \tag{6.7}$$

and

$$\bar{R} = \frac{2L\Pi v_w}{T_w} = \frac{2L^2 n_c^2 \delta^2}{\pi\eta}\left(1 - \frac{\eta}{n_c L}\right)^{-1} \times \left(\int_0^\pi f_1(\theta) \sin^2\theta\, d\theta\right)^2 + o(\delta^2) \tag{6.8}$$

The expression for $\bar{M}$ in (6.3) in terms of δ and L is

$$\bar{M} = \frac{2L^2 n_c^2 \delta^2}{\pi\eta}\left(\int_0^\pi f_1(\theta) \sin^2\theta\, d\theta\right)^2 + \frac{1}{2} L n_c \delta^2 \left(1 - \frac{\eta}{n_c L}\right) \times \int_0^\pi \{f_1^2(\theta) \sin^{-1}\theta + [f_1'(\theta)]^2 \sin\theta\}\, d\theta + o(\delta^2) \tag{6.9}$$

Comparing (6.8) to (6.9), we see that the term of $\bar{M}$ proportional to L^2 coincides with the corresponding term of $\bar{R}$, while the terms of order L differ. The difference between $\bar{M}$ and $\bar{R}$ thus gets relatively small as L increases, with the value of $\bar{M}$ remaining slightly larger than the value of $\bar{R}$ as $\delta \to 0$. This is in agreement with the computer simulations.

We now calculate $\bar{M}$ for our model, where, according to (5.9), $f_1(\varphi) = -\varphi$ and $f_2(\varphi) \equiv 0$. The expansion (6.1) now has a singular term and so we need to use the original formula (5.2)

$$\bar{M} = -2Ln_c\{\ln(1-\delta) + \langle \ln\sin[(1-\delta)\varphi]\rangle - \langle \ln\sin\varphi\rangle\}$$

$$= -2Ln_c(I_0 + I_1 - I_2) \tag{6.10}$$

where $I_0 = -\delta + O(\delta^2)$ and the two other terms involve integration with respect to the density (6.2). It will be sufficient to integrate only with the

zeroth-order terms there since corrections will, as before, produce terms of order δ^2, which we can now disregard compared to the leading term. We find

$$I_2 = \langle \ln \sin \varphi \rangle = \tfrac{1}{2} \int_0^\pi \sin \theta \ln \sin \theta \, d\theta = \ln 2 - 1 \tag{6.11}$$

and

$$I_1 = \langle \ln \sin[(1-\delta)\varphi] \rangle = \tfrac{1}{2} \int_0^\pi \sin \theta \ln \sin[(1-\delta)\theta] \, d\theta \tag{6.12}$$

This yields

$$I_1 = \ln 2 - 1 + \delta + \frac{\pi^2}{4} \delta^2 \ln \delta + O(\delta^2) \tag{6.13}$$

Combining the expansions for I_0, I_1, and I_2 gives

$$\bar{M} = -2^{-1} \pi^2 L n_c \delta^2 \ln \delta + O(\delta^2) \tag{6.14}$$

The corresponding expression for $\bar{R}$ has no singular terms,

$$\bar{R} = \frac{\pi^3 L^2 n_c^2}{8\eta} \left(1 - \frac{\eta}{n_c L}\right) \delta^2 + o(\delta^2) \tag{6.15}$$

This gives

$$\bar{M}/\bar{R} = \text{const} \ln(1/\delta) + O(1) \to \infty \tag{6.16}$$

In other words, for our c-model, when L is finite and $\delta \to 0$, the quantities $\bar{M}$ and $\bar{R}$ have different rates of convergence to zero!

Remark. We also calculated the second-order term in the expansion of $\bar{M}$:

$$\bar{M} = -2^{-1} \pi^2 L n_c \delta^2 \ln \delta + C_2 \delta^2 + O(\delta^3) \tag{6.17}$$

where

$$C_2 = \frac{\pi^3 n_c^2 L^2}{8\eta} - 11.9202 n_c L \tag{6.18}$$

7. NUMERICAL RESULTS

Computer simulations for our b- and c-models were performed with $N=100$ and $N=200$ hard disks of unit mass and diameter $\sigma=1$. We kept the volume fraction occupied by the disks, $\pi\bar{n}/4$, equal to 0.1. Our system was thus in the dilute-gas phase. For $N=100$ this corresponds to $L=28.0$ and for $N=200$ to $L=39.6$. The mean free path l at this density is about 2.3,[27] so $L/l\sim 17$ for the latter. (Discrepancies between results of the simulations and of hydrodynamics can therefore be expected *a priori* to be of order $2u_h/17$.)

The positions of the particle centers were chosen randomly (without overlap) in a domain $|x|\leqslant L/2$, $|y|\leqslant(L-1)/2$. The initial velocities were generated randomly with subsequent normalization of the total kinetic energy so that $2E=\sum v_i^2=N$.

There is an obvious instability in the dynamics, and the round off errors accumulate at an exponential rate. In fact, the system loses its memory completely after every 100–200 collisions in the box. The dynamical meaning of computer simulations of unstable dynamical systems like ours is a difficult question, which has been discussed recently in the literature.[28] One way to think of roundoff errors is a small perturbations of the deterministic trajectory of the phase point made at every collision. So, instead of a true trajectory, we can only track a perturbed one, or a pseudotrajectory. Then the question is—what are the quantities measured by averaging along such pseudotrajectories?

One possible answer is given by the so-called shadowing lemma[29] (for discontinuous dynamics see ref. 30). It says that for smooth hyperbolic systems every pseudotrajectory is shadowed (approximated) by a real trajectory. The distance between the two trajectories is of the order of the computer accuracy. This may justify averaging over computer-generated pseudotrajectories for smooth hyperbolic systems, although it certainly does not guarantee that these finite-time averages represent typical behavior.[28] Moreover, our dynamics is not smooth, and hyperbolicity cannot be easily established. Trust in the results of our simulations, like all others done on such unstable dynamical systems, therefore relies mainly on faith in some kind of typicality resulting from the (pseudo) random effects of the roundoffs.[28]

In any case, to prevent the system from leaving the energy surface due to roundoff errors, the total kinetic energy was renormalized after every N collisions in the box.

With the above reservations we believe that the results to be described are statistically reliable within 1%. This is based on various checks comparing different runs and different levels of computer precision. For each

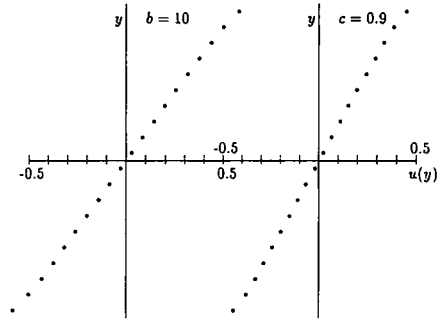

Fig. 1. Velocity profiles $u(y)$ for the models $b = 10$ and $c = 0.9$.

value of b and c we averaged over about 25,000 collisions per particle with other particles and about 1200 with the walls. We also changed the computer precision from single (7 accurate decimals) to double (14 decimals) and the so-called long double (19 decimals) to make sure the results were stable. Most of the programming was done in the C language on an 80486/DX-66 PC and on a SUN SPARC station 1000 at the University of Alabama at Birmingham.

In each run the vertical height occupied by the centers $L-1$ was divided into 20 equally spaced horizontal layers and time averages of the density $n(y)$, mean x-velocity $u(y)$, and variances $\langle (v_x - u)^2 \rangle$ and $\langle v_y^2 \rangle$ were taken. We also recorded time averages of x-momentum transfer from the walls Π and the compression rate M.

Figures 1 and 2 show typical velocity and temperature profiles $u(y)$ for the b- and c-models with $N = 200$ particles. The velocity profiles are almost linear and the temperature profiles $T(y) = \frac{1}{2}\langle [v_x - u(y)]^2 + v_y^2 \rangle$ almost quadratic, away from the walls, consistent with the approximation (3.6).

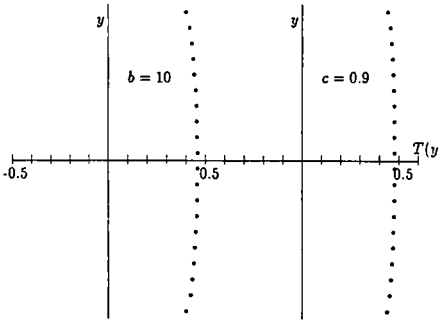

Fig. 2. Temperature profiles $T(y)$ for the models $b = 10$ and $c = 0.9$.

The deviations from linearity near the walls are due to the dependence of both η and κ on T and n, which means that we should use (3.3) rather than use (3.6). Since $\eta(n, T) \sim \sqrt{T}$, this will indeed lead to increases in the slope near the wall. There are of course also effects due to deviations from the hydrodynamic limit of $O(2u_b l/L)$, but these are harder to compute.

We estimated the shear rate $du(y)/dy$ by the least square fir of a line $u(y) = \gamma y$ to the experimental velocity profile and used the experimental momentum transfer from wall to wall Π to find the average shear viscosity as defined in (3.4), $\bar{\eta} = \Pi/\gamma$. To mitigate the problem arising from the nonlinearity of the profile near the wall, we used only the data in the bulk of the system, from level 4 to level 17, i.e., we excluded the top three and the bottom three levels. Table I presents the experimental values of the shear viscosity computed for the b- and c-dynamics with $N = 200$ particles. The essentially linear dependence of Π on δ is certainly consistent with (6.6).

The shear viscosity of hard-disk fluids can be estimated via Enskog's modification of the Boltzmann equation.[31,32] It gives the value

$$\eta_E = \eta^{\text{dilute}}[\chi^{-1} + bn + 0.8729\chi(bn)^2] \tag{7.1}$$

where η_{dilute} is the value obtained from the Boltzmann equation[31]

$$\eta_{\text{dilute}} = 1.022 \frac{1}{2}\sqrt{\frac{kT}{\pi}} \tag{7.2}$$

for disks of unit mass and diameter. In (7.1) b is the second virial coefficient, $b = \pi/2$, and χ is the Enskog scaling factor, which is just the

Table I. Computed and Theoretical Values of η

Model	Π_{exp}	η_{exp}	Enskog η
$b = 10$	6.03×10^{-3}	0.204	0.209
$b = 25$	3.12×10^{-3}	0.213	0.219
$b = 50$	1.66×10^{-3}	0.221	0.222
$b = 100$	0.85×10^{-3}	0.218	0.222
$b = 200$	0.43×10^{-3}	0.216	0.222
$c = 0.90$	4.87×10^{-3}	0.213	0.214
$c = 0.95$	2.82×10^{-3}	0.221	0.220
$c = 0.97$	1.77×10^{-3}	0.206	0.221
$c = 0.99$	0.62×10^{-3}	0.229	0.222

equilibrium pair-correlation function at contact. We have estimated χ by using the pressure equation for hard-disk fluids,

$$\frac{p}{nkT} = 1 + \frac{\pi}{2} n\chi \tag{7.3}$$

and its virial expansion in the number density n, or equivalently the "scaled particle" approximation[34,35]

$$p/nkT = 1 + bn + b_3 n^2 + b_4 n^3 + \ldots \approx (1 - \pi n/4)^{-2} \tag{7.4}$$

In our case $bn = 0.2$, and we get

$$\eta_E \approx 1.081 \eta_{\text{dilute}} \tag{7.5}$$

The value of η_E so computed using the measured mean temperature and density in rows 4–17 is shown in the last column of Table I. The agreement is very good, as would be expected for the low-density system we are considering.

We next checked the constancy of the pressure $p(n, T)$. To do this, it is important to note that Eq. (7.3) is valid, even for uniform equilibrium systems, *only* in the bulk, i.e., at distances from the wall large compared to the equilibrium correlation length. For our dilute-gas system this length is of order $\sigma = 1$. Near the wall the density becomes nonuniform, with the density *at the wall* n_w equal to p/kT; T is the uniform equilibrium temperature.[31] Since the hydrodynamic equations (3.1) are valid on a scale which is very large compared to any microscopic scale, this variation in density is not considered there. The situation is very different, however, for our computer simulations, where we can expect to see these density variations.[19] Indeed, the pressure defined as the average y-momentum transfer from the top wall in the y direction per unit length and unit time would be, using (5.3), in analogy to (5.6), equal to $n_c \langle r(\sin f(\theta) + \sin\theta) \rangle$. This would reduce to $n_w kT$ to zeroth oder in δ.

We present in Table II experimental values of n, T, as well as the bulk pressure defined in (7.3) in the different layers, taking the man of the values in the layers situated symmetrically about the middle. Here the density is given by the average number of particles on each level. Since $n(y)$ increases rapidly as we approach the wall, we do not have a simple formula for p in the top column. Using $n_w = p/kT$ leads to an extrapolated density at the wall of about 13.4 and 13 for the $b = 10$ and $c = 0.9$ cases, respectively.

The agreement between the prediction of the hydrodynamic equation (3.6) and the simulation results shows that the Maxwell-demon boundary drives indeed set up, in the limit $L \to \infty$, an MSNS for shear flow. We

Table II. Experimental Measurements of the x Velocity, Temperature T, Density n, and Pressure p on All Levels for the $b=0$ and $c=0.9$ Models

	$b=10$				$c=0.9$			
Level	v_x	T	n	p	v_x	T	n	p
1	0.584	0.399	11.35	—	0.449	0.439	10.70	—
2	0.502	0.420	10.35	5.330	0.383	0.453	10.15	5.722
3	0.437	0.430	10.13	5.338	0.333	0.459	10.06	5.724
4	0.374	0.438	9.97	5.337	0.289	0.465	9.94	5.713
5	0.315	0.443	9.86	5.331	0.244	0.469	9.89	5.712
6	0.257	0.449	9.77	5.341	0.197	0.471	9.85	5.713
7	0.198	0.454	9.67	5.341	0.153	0.473	9.84	5.715
8	0.141	0.455	9.67	5.342	0.111	0.474	9.82	5.720
9	0.084	0.457	9.63	5.344	0.067	0.475	9.82	5.718
10	0.028	0.459	9.60	5.340	0.022	0.476	9.80	5.714

therefore computed the values of $\bar{R}$ and $\bar{M}$ defined for our shear flow by formulas (5.2) and (4.2) with Π given by (5.5) experimentally, by using time averages of the appropriate dynamical functions in our simulations. We also computed these quantities numerically according to our integral formulas using the Maxwellian ansatz (5.4). In both these computations we used the experimental values of T_w, v_w, and n_c. The results are presented in Table III. The last column of Table III gives the leading term in δ, computed from (5.12), for which $\bar{M}=\bar{R}$.

The agreement between the so-computed theoretical values of $\bar{M}$ and $\bar{R}$ and their experimental values is quite good. This suggests that the integral formulas (5.6) and (5.2) with the Maxwellian density (5.4) are quite accurate.

We also tested directly this hypothesis using a chi-square test and the Kolmogorov–Smirnov test (see, e.g., ref. 37). Both tests accepted the

Table III. The Experimental and Theoretical Values of M and R

Model	$M_{\text{th}}/M_{\text{exp}}$	$R_{\text{th}}/R_{\text{exp}}$	M_{lead}
$b=10$	0.761/0.740	0.695/0.767	0.867
$b=25$	0.161/0.157	0.156/0.162	0.169
$b=50$	0.0429/0.0417	0.0422/0.0428	0.0437
$b=100$	0.0113/0.0110	0.0111/0.0112	0.0113
$b=200$	0.00294/0.00285	0.00289/0.00289	0.00291
$c=0.9$	0.448/0.444	0.405/0.432	0.402
$c=0.95$	0.149/0.148	0.127/0.131	0.126
$c=0.97$	0.0641/0.0632	0.0523/0.0531	0.0518
$c=0.99$	0.00871/0.00868	0.00628/0.00632	0.00625

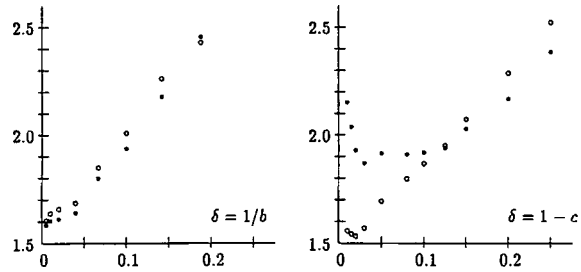

Fig. 3. The ratios M/v_w^2 (solid circles) and R/v_w^2 (open circles) versus $\delta = 1/b$ and $\delta = 1 - c$.

distribution (5.3) for the velocity vectors of incoming particle colliding with the wall for various values of b and c. Just to determine the sensitivity of our procedure, we tested in the same way the distribution of the *outgoing* velocity vectors [whose Maxwellianity would contradict our assumption (5.3)]. As expected, both tests frequently rejected this last hypothesis for several values of b and c, indicating that the reflection rule (2.1) distorts the velocity distribution in a considerable way even for small δ.

Remarks. (1) Our analysis in Section 6 shows that the quantities $\bar{M}$ and $\bar{R}$ are of order v_w^2 as $\delta \to 0$, with the exception of $\bar{M}$ for the c-model, which is of order $v_w^2 \ln(1/v_w)$. Figure 3 shows the ratios M/v_w^2 and R/v_w^2 as functions of δ. For the b-model they both "nicely" converge to the same positive constant (≈ 1.6) as $\delta \to 0$. For the c-model the ratio R/v_w^2 also converges to a number (≈ 1.55), while M/v_w^2 apparently grows to infinity, in agreement with the prediction in Section 6.

(2) An interesting question is how the velocity near the wall v_w depends on the model parameter δ as the size L is held fixed and δ is not very small. Figure 4 shows the experimental values of v_w versus δ as δ varies between zero and 0.5. A linear regression for small δ is very clear for

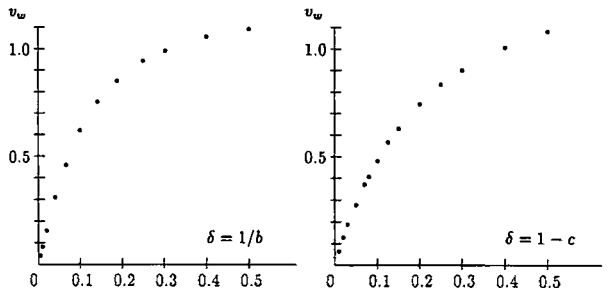

Fig. 4. The velocity v_w near the wall versus $\delta = 1/b$ and $\delta = 1 - c$.

both models. For large δ, the function $v_w(\delta)$ increases more and more slowly, and apparently has a finite asymptote $v_w(+\infty)$. This happens for a simple reason—the energy balance in the system. Given a linear velocity profile $u(y) = \gamma y$, the energy balance with the minimal temperature $T(y) \equiv 0$ gives $\gamma_{\max} = \sqrt{6}/L$, so that

$$v_{w,\max} = \sqrt{6}/2 \approx 1.225 \tag{7.6}$$

Indeed, the largest velocity near the wall we observed in our simulations (say, with $b = 0$ or $c = 0.2$) was around 1.2. Under these conditions, however, the laminar velocity profile breaks down.

8. DISCUSSION

In Section 5 we obtained an equality between the phase-volume contraction $\bar{M}$ defined in (5.2) for the mSNS produced by our model and the hydrodynamic entropy production $\bar{R}$ defined in (4.2) for the MSNS, in the limit $L \to \infty$, $\delta \to 0$, with $\delta L = a$ fixed. To understand the origin of this equality, also found approximately in our computer simulations, we will analyze here in more detail the production of entropy in nonequilibrium macroscopic systems discussed in Section 4 for SNS. This will use formal manipulations of various expressions for the entropy of such systems whose justification requires, at the minimum, the validity of dissipative hydrodynamics, e.g., the Navier–Stokes equations of Section 3, obtained as a scaling limit in going from microscopic to macroscopic descriptions of our system. It will assume *ipso facto* the existence of LTE in these systems, since this is required for the derivation of the hydrodynamic equations.[11] While these assumptions are very reasonable for systems not too far from equilibrium, where the interactions (collisions) between the particles, tending to bring the system to equilibrium, dominate locally over the external forces and fluxes pushing the system away from equilibrium, such results are *very far* from being proven for systems with Hamiltonian dynamics. Even their derivative from the Boltzmann equation is still incomplete.[24] Given this situation, there seems little point in giving any proofs here—even for those parts where this may be possible. Instead the analysis should be thought of as heuristic and suggestive.

For a system in LTE with hydrodynamic variables $n(\mathbf{r}, t)$, $\mathbf{u}(\mathbf{r}, t)$, and $e(\mathbf{r}, t)$, corresponding to particle density, velocity, and energy density, respectively, evolving according to hydrodynamic equations, the hydrodynamic entropy S_h of the system at any time t is the integral of $s_{eq}(n, e')$,

the entropy density in a *uniform* equilibrium system with densities n and e',[1,11,25]

$$S_h \equiv \int_{\text{Volume}} s_{\text{eq}}(n(\mathbf{r}), e'(\mathbf{r}))\, d\mathbf{r} \tag{8.1}$$

where $e'(\mathbf{r}) \equiv [e(\mathbf{r}) - \frac{1}{2}n(\mathbf{r})\,\mathbf{u}^2(r)]$ is the thermal energy density. For an equilibrium system, $\mathbf{u}$ has to be independent of $\mathbf{r}$ and can therefore be removed by a Galilean transformation.

We also have, essentially from the definition of LTE, that macroscopic systems in LTE have a *local* microscopic description which is, to leading order, the same as that for a *uniform* equilibrium system with the same parameters; i.e., if we consider a "small" *macroscopic volume element* around $\mathbf{r}$, its properties will be approximately given by the grand-canonical ensemble, assumed to be equivalent to the canonical or microcanonical ensemble, specified by the local values of n, $\mathbf{u}$, and e, at time t.[11,35] The dissipative fluxes are then related by the transport coefficients to the gradients of the hydrodynamic variables, which are very small on the microscale.

Let us call $\mathscr{M}$ the macroscopic state specified by the hydrodynamic variables $\{n, \mathbf{u}, e\}$ and let $\nu(X; \mathscr{M})$ be the grand canonical ensemble with *local* chemical potential and temperature appropriate to $n(\mathbf{r})$, $e'(\mathbf{r})$. Then we have that S_h is equal to the Gibbs entropy S_G defined in (4.4), corresponding to $\mu = \nu$,[11,25,35]

$$S_h \simeq S_G(\nu) \equiv -\int \nu(X; \mathscr{M}) \log \nu(X; \mathscr{M})\, dX \tag{8.2}$$

It is furthermore true, as observed by Boltzmann, that the hydrodynamic entropy S_h of a system in the macrostate $\mathscr{M}$ is equal to the logarithm of the phase-space volume $\Gamma(\mathscr{M})$ associated with the macroscopic state $\mathscr{M} = \{n, \mathbf{u}, e\}$,[26] i.e.,

$$S_h \simeq S_B(\mathscr{M}) \equiv \log \Gamma(\mathscr{M}) \tag{8.3}$$

[Note that $S_B(\mathscr{M})$ may make sense even when $\mathscr{M}$ does not correspond to an LTE state, when S_h is not well defined. We shall not consider such cases here, however, so (8.3) will always hold.]

The equality between the different expressions for the macroscopic entropy of systems in LTE given in (8.1)–(8.3) depends crucially on the large separation of scales between the micro and macro descriptions. It holds to leading order in the ratio of micro- to macroscales, e.g., l/L

defined in Section 7, and becomes exact, in the sense that it has the same limiting value when divided by the number of particles in the system, only when the ratio of micro- to macroscales goes to zero, the hydrodynamic scaling limit. For real systems the equality is only approximate, as are the hydrodynamic equations, etc. We shall, however, following Newton in a different but similar context,[36] assume that "the error will not be sensible; and therefore this ... may be considered *as physically exact*" (italics added) and will therefore treat (8.2) and (8.3) as true equalities.

Taking the time derivative of (8.1) using the standard equilibrium relations for derivatives of s_{eq}, we obtain

$$\dot{S}_h = \int_{\text{Volume}} \left\{ -\frac{\lambda}{T}\frac{\partial n}{\partial t} + \frac{1}{T}\left[\frac{\partial e}{\partial t} - \frac{\partial}{\partial t}\left(\frac{1}{2}nu^2\right)\right]\right\} d\mathbf{r} \tag{8.4}$$

where $\lambda(\mathbf{r}, t)$ is the local chemical potential and $T(\mathbf{r}, t)$ the local temperature. The integrand in (8.4) can be rewritten as

$$\frac{\partial s_{eq}}{\partial t} = -\frac{\partial}{\partial \mathbf{r}} \cdot \mathbf{j}_s(\mathbf{r}, t) + \sigma(\mathbf{r}, t)$$

where $\mathbf{j}_s$ is the entropy flux and $\sigma(\mathbf{r}, t)$ is the local entropy production. The latter can be written in a form similar to (4.1) in terms of the full pressure tensor $\mathbf{P}(\mathbf{r}, t)$, heat flux $\mathbf{J}(\mathbf{r}, t)$, etc., and is nonnegative by the second law.[1,17,35] We thus find

$$\dot{S}_h(t) + \int_{\text{Surface}} \mathbf{j}_s(\mathbf{r}, t) \cdot \mathbf{ds} = \int_{\text{Volume}} \sigma(\mathbf{r}, t)\, d\mathbf{r} \equiv R_I(t) \geqslant 0 \tag{8.5}$$

For an *isolated* macroscopic system the integral of $\mathbf{j}_s$ over the surface vanishes and the rate of change of $S_h(t)$ is then given by $R_I(t)$. We can thus interpret R_I as the rate at which S_B is produced inside the system when it is in LTE (LTE was implicitly assumed in Sections 3 and 4.1). Furthermore, since the system is isolated, we expect it to approach, as $t \to \infty$, a uniform global equilibrium state, with $S_h \to S_{eq} = (\text{Volume}) \cdot s_{eq}(\bar{n}, \bar{e})$ and $R_I \to 0$.

Consider next the hydrodynamic description of an "open" macroscopic system subjected to external forces and able to exchange heat through its surface with k heat baths maintained at temperatures T_α, $\alpha = 1,..., k$. (In the shear flow case we could have the walls at different temperatures.) We will now have, using (8.5) for the time derivative of the system's hydrodynamic entropy, assuming that the part of the system in

contact with the αth heat bath has a temperature very close to T_α (we are considering for simplicity the "no-slip" vase),

$$\dot{S}_h(t) = R_I(t) - \sum J_\alpha(t)/T_\alpha \tag{8.6}$$

Here J_α is the heat flux from the system to the αth heat bath, i.e., J_α/T_α is the net hydrodynamic entropy flux leaving the system through that part of the surface which is at temperature T_α. Thus J_α/T_α is analogous to the equilibrium relation $dS = dQ/T$ extended to quasistationary processes; see in particular Chapter 14 in Balian's book.[1] Note that, in accordance with (8.2), the external mechanical forces do not contribute directly to the entropy change, as they do not, by Liouville's theorem, change the phase-space volume $\Gamma(\mathscr{M})$ available to the macrostate $\mathscr{M}$.

When the differences in the T_α and the magnitude of the external forces are not too large we expect this system to come to a stationary LTE state in which $\dot{S}_h$ vanishes, with

$$R_I \to \bar{R}_I = \sum \bar{J}_\alpha/T_\alpha \tag{8.7}$$

in accord with (4.2), for laminar shear flow.

Let us investigate now the statistical microscopic description of these macroscopic situations. Following the usual procedures of statistical mechanics for macroscopic systems, we represent their macroscopic state $\mathscr{M}$ at time t by a suitable ensemble density $\mu(X, t)$. This μ is assumed to have the property that the hydrodynamic variables $\mathscr{M}_{\mu_t} = \{n, \mathbf{u}, e\}$ obtained as expectation value with respect to $\mu(X, t)$ of the corresponding phase-space functions are sharply defined (very little dispersion with respect to μ), vary slowly in space and time on the microscopic scales, and evolve, on the appropriate macroscopic scales, accoding to the hydrodynamic equations. We will associate to $\mu(X, t) \equiv \mu_t(X)$ the local equilibrium ensemble density $\nu(X|\mathscr{M}_{\mu_t})$ and, with some abuse of notation, shall set $\nu(X|\mathscr{M}_{\mu_t}) = \nu_t(X)$. *N.B.*: While we assume that our system is in LTE, we are *not* assuming here that $\mu_t = \nu_t$.

We now take the Gibbs entropy S_G of the ensemble density μ_t defined in (4.4) and split in into two parts,

$$\begin{aligned} S_G(\mu_t) \equiv S_G(t) &\equiv -\int \mu_t(X) \log \mu_t(X)\, dX \\ &= -\int \mu_t(X) \log[\mu_t(X)/\nu_t(X)]\, dX \\ &\quad + \int \mu_t(X) \log \nu_t(X)\, dX \end{aligned} \tag{8.8}$$

The first term on the right side of (8.8) is the relative entropy of μ_t with respect to ν_t (which is negative, or zero, by convexity of $x \log x$). To evaluate the second term, we use the fact that, by the definition of ν, as a locally grand-canonical ensemble density, $\log \nu(X)$ is a function of X whose average is expressible in terms of $\mathcal{M} = \{n, \mathbf{u}, e\}$. Now, by the definition of ν_t these are the actual hydrodynamic variables in our system, so that the second term is equal to $\int \nu_t(X) \log \nu_t(X)\, dX$. Hence the second term in (8.8) is, using (8.2), equal to $S_h(t)$, and we therefore have that

$$S_G(t) = S_G(\mu_t \mid \nu_t) + S_h(t) \tag{8.9}$$

Equation (8.9), which is valid for all macroscopic systems in LTE, gives an important connection between S_G and S_h for such systems.

For an isolated system with a given Hamiltonian H, we write $\dot{X} = \mathscr{F}_H(X)$ for the flow in the phase space. The ensemble density $\mu(X, t)$ then evolves according to the Liouville equation,

$$\frac{\partial \mu(X, t)}{\partial t} = \mathscr{L}_H \mu = -\operatorname{div}(\mu \mathscr{F}_H) = -\nabla \mu \cdot \mathscr{F}_H \tag{8.10}$$

subject to some initial condition $\mu(x, 0) = \mu_0(X)$. (We think of $X, \mathscr{F}, \nabla$ as $2dN$-dimensional vectors in the phase space and in the lst equlity used the fact that $\operatorname{div} \mathscr{F}_H = 0$.) As was already known to Gibbs, and is proven in almost every textbook on statistical mechanics, $S_G(t)$ is constant in time for an isolated system. Hence, using (8.9), we have

$$\dot{S}_G(t) = \dot{S}_G(\mu_t \mid \nu_t) + \dot{S}_h(t) = 0 \tag{8.11}$$

or

$$\dot{S}_G(\mu_t \mid \nu_t) = -\dot{S}_h(t) = -R_t(t) \tag{8.12}$$

Note that in going from (8.11) to (8.12) we are glossing over the difference between microscopic and macroscopic time scales.[11,25,35] In the same spirit we will also have that $R_t(t) = \langle \tilde{R}_t \rangle$, where R_t is a suitable microscopic function and the average is with respect to μ_t, not ν_t.

As $t \to \infty$, we expect that μ_t and ν_t will both "approach" the Gibbs distribution μ_{eq} appropriate for a macroscopic system in equilibrium with a uniform temperature and density. Note, however, that while $S_h(t)$ approaches S_{eq}, the Gibbs entropy $S_G(\mu_t)$, being constant, clearly does not. Hence if $\mu_0(X)$ is not an equilibrium state, the limit, as $t \to \infty$, of $S_G(\mu_t \mid \nu_t)$ will be $S_G(0) - S_{eq}$, which is negative and can be large, i.e., extensive, indicating the "entanglement" of $\mu_t(X)$ necessary to keep S_G constant.

An explicit example where $S_G(\mu_t \mid \nu_t)$ can be shown to be extensive for large t occurs for noninteracting point particles moving among a periodic set of fixed scatterers, the periodic Lorentz gas or Sinai billiard, which are started at $t=0$ in a product measure with the same energy (speed) and a macroscopically *nonuniform* density. The density then evolves on the macroscopic scale according to the diffusion equation (see refs. 11 and 25 and references therein. This leads to a uniformization of the density and an increase in $S_h(t)$, while $S_G(t)$ remains constant. The entanglement of $\mu_t(X)$ corresponds here to the build up to correlations between the positions and velocities of the particles in the system as it evolves toward a spatially uniform state. (The lack of interaction between the particles makes this system a bit unphysical.)

We turn now to the statistical mechanics of open systems, e.g., a fluid with shear flow, whose macroscopic behavior is described by the compressible Navier–Stokes equations Modeling such a system microscopically as one driven by stochastic thermal reservoirs and some external forces, e.g., rough walls with constant temperatures and velocities, as in Section 4.2, we obtain the time evolution of $\mu(X, t)$ as[4,5]

$$\frac{\partial \mu}{\partial t} = (\mathscr{L}_H + \mathscr{L}_{ex} + \sum \mathscr{K}_\alpha)\,\mu \tag{8.13}$$

Here $\mathscr{K}_\alpha$ represents the stochastic effect of the αth reservoir, which tries to bring the system to equilibrium with a temperature T_α, and $\mathscr{L}_{ex}\mu = -\mathscr{F}_{ex}\nabla\mu$, assuming that the external foce $\mathscr{F}_{ex}$ is (phase-space) divergence-free. The Gibbs entropy $S_G(t)$ will no longer be constant in time, so (8.12) will no longer hold. Assuming the system to be in LTE, we shall have instead of (8.12) the behavior given in (8.6), with

$$\dot{S}_h(t) = \langle \tilde{R}_t \rangle - \sum \langle \tilde{J}_\alpha \rangle / T_\alpha \tag{8.14}$$

where $\langle \cdot \rangle$ is the average with respect to $\mu(X, t)$ of the phase-space functions $\tilde{R}_t$ and $\tilde{J}_\alpha$; $\tilde{J}_\alpha$ specifies the rate at which energy flows from the system to the αth reservoir. As in (8.6), we are ssuming here that in our system the spatial region in contact with the αth reservoir is itself at a temperature very close to T_α. [Compare (8.14) with (4.3), where there is no assumption of LTE; $\mathscr{R}$ there corresponds to $\dot{S}_G(\mu_t \mid \nu_t) + R_t$.]

We may assume that our ensemble density $\mu(X, t)$, evolving according to (8.13), will, in contrast to what happens in an isolated system, approach a smooth stationary density $\bar{\mu}(X)$, while $\nu_t(X) \to \bar{\nu}(X) = \nu(X \mid \mathscr{M}_\mu)$.[4,5,10]

Thus, for $t \to \infty$, $S_h(t)$ will approach the hydrodynamic entropy $\bar{S}_h$ in the MSNS, which according to (8.2) is given by

$$\bar{S}_h = -\int \bar{\nu}(X) \log \bar{\nu}(X)\, dX \tag{8.15}$$

Setting $\dot{S}_B(t) = 0$, in (8.14) and letting $\bar{R}_I$ be the internal entropy production in the stationary state, we have

$$\bar{R}_I = \sum \langle \tilde{J}_\alpha \rangle_\mu / T_\alpha \tag{8.16}$$

Comparing (8.16) with (8.7), we can identify the average of $\tilde{J}_\alpha$ with respect to $\bar{\mu}$, $\langle \tilde{J}_\alpha \rangle_{\bar{\mu}}$, with the hydrodynamic steady-state energy flux $\bar{J}_\alpha$, which, for a system in LTE, should be just $\langle \tilde{J}_\alpha \rangle_{\bar{\nu}}$. Since we further expect that the stochasticity of the reservoirs will make the stationary $\bar{\mu}$ a "smooth" density, independent of the initial μ_0, we should also have here

$$\dot{S}_G(t) \to 0, \qquad S_G(\mu_t \mid \nu_t) \to S_G(\bar{\mu} \mid \bar{\nu}) \qquad \text{for} \quad t \to \infty \tag{8.17}$$

Let us turn now to the microscopic modeling of the open macroscopic systems by "thermostatted" deterministic forces $\mathscr{F}_{ts}(X)$ which conserve the energy but whose divergence does not vanish, e.g., the Maxwell-demon boundary drives discussed in this paper. For the sake of simplicity we shall treat $\mathscr{F}_{ts}(X)$ as if it were smooth, but think of it as acting only in the vicinity of the boundaries; the transition to a boundary term should then be possible (see the Appendix). The time evolution of a microstate X will now be given by the deterministic equation

$$\dot{X} = \mathscr{F}_H(X) + \mathscr{F}_{ts}(X) \tag{8.18}$$

and that of $\mu(X, t)$ by

$$\frac{\partial \mu}{\partial t} = -\operatorname{div}[(\mathscr{F}_H + \mathscr{F}_{ts})\,\mu] \tag{8.19}$$

Taking the time derivative of $S_G(t)$, we get, as in (4.6),

$$\dot{S}_G(t) = \int \mu_t(X) \operatorname{div} \mathscr{F}_{ts}(X)\, dX \equiv -M(t) \tag{8.20}$$

We also have, using (8.8) and (8.9), for systems in LTE, that

$$\dot{S}_h(r) = \frac{d}{dt}\int \mu_l(X) \log \nu_l(X)\, dx$$

$$= -\int \mathscr{F}_H(\nabla \cdot \mu_l) \log \nu_l\, dx$$

$$-\int \operatorname{div}(\mathscr{F}_{ts})\, \mu_l \log \nu_l\, dx - \int \mu_l(X) \frac{\partial}{\partial t} \log \nu_l(X)\, dX \qquad (8.21)$$

In the last term on the rhs of (8.21) we can replace μ_l by ν_l since the time derivative of $\log \nu_l$ at a fixed X involves only phase-space functions whose expectation corresponds to the hydrodynamic variables. After this replacement the last term becomes $(d/dt)\int \nu_l(X)\, dX$, which vanishes by normalization. We are thus left with

$$\dot{S}_h(t) = -\int (\mathscr{F}_H \cdot \nabla \mu_l) \log \nu_l\, dX + \int \mu_l \mathscr{F}_{ts} \cdot \nabla \log \nu_l\, dX \qquad (8.22)$$

We now want to argue that for "smooth" thermostatted forces we can again replace μ_l by ν_l in the last term in (8.22), obtaining

$$\int \nu_l \mathscr{F}_{ts} \cdot \nabla \log \nu_l\, dX = -\int \mathscr{F}_{ts} \cdot \nabla \nu_l\, dX$$

$$= \int \nu_l \operatorname{div} \mathscr{F}_{ts}\, dX \equiv -M_l(t) \qquad (8.23)$$

We also argue that then first term on the right side of (8.22), which is the only term present in an isolated system, is just $R_l(t)$. Accepting these "arguments," we finally get for systems with thermostatted forces in LTE

$$\dot{S}_h(t) = R_l(t) - M_l(t) \qquad (8.24)$$

We note that (8.24) gives a decomposition of the rare of change of S_h into an internal part R_l coming from the dissipative fluxes inside the system and a thermostatted part $-M_l$ coming from the thermostat forces $\mathscr{F}_{ts}$. Comparing this with (8.4) and remembering that $\mathscr{F}_{ts}$ does not change n or e, we have that M_l will contribute only to the lst term there,

$$-\int \frac{1}{T}\frac{\partial}{\partial t}\left(\frac{1}{2} m u^2\right) d\mathbf{r}$$

In fact, M_l corresponds to the surface term in (8.5), which for the models considered in this paper is equivalent to the second term on the right side of (8.6): it represents the production (or reduction) of S_h due to the conversion of thermal into directed energy by the Maxwell demons producing the $\mathscr{F}_{ts}$ at the boundary.

Interestingly, the contribution of the $\mathscr{F}_{ts}$ to $\dot{S}_h$, $-M_l(t)$, is just the rate of change of $S_G(t)$ *when* $\mu_l = \nu_l$. It is tempting to try and bypass the formal manipulations leading to (8.24) and derive that relation more directly from the definition of $S_B(\mathscr{M})$ in (8.3) as $\log \Gamma(\mathscr{M})$, but we have not yet succeeded in doing this.

Waiting now for a time $\bar{t}$ which is long enough for the system to become approximately stationary on the macroscopic level, we would have $\dot{S}_h(t) \approx 0$ for $t \geqslant \bar{t}$, and thus

$$\bar{R}_l = \bar{M}_l \tag{8.25}$$

Equation (8.25) explains the equality between (5.12) and (5.15). *If* it is further true that div $\dot{X}$ is sufficiently smooth for its average to be well approximated by M_l, then we would have $\bar{M} = \bar{M}_l = \bar{R}_l$. This appears to be the case in many situations, including the Maxwell-demon boundaries considered in this paper, where div $\dot{X}$ is an additive function of the coordinates and velocities of each particle so that its average M depends only on the one-particle distribution function at the wall. This leads to $\bar{M} \approx \bar{R}_l$, which we observe in our simulations. We actually expect the equality (8.25) to hold for general thermostatted SNS *as long as* LTE *holds* in the SNS. It should in particular hold for macroscopic fluids driven by rules (2.3) or (2.4) even when the flow is no longer laminar. We hope to test this via simulations on large systems.

APPENDIX. SPECIAL REFLECTION RULES

It seems reasonable to expect that time-reversible reflection rules, like rule b, can be obtained as limits of the usual smooth Gaussian thermostatted dynamics.[7,8] We describe here a very simple example of such a limit which also provides an illustration of the relation between $\bar{M}_l$ and $\bar{R}_l$, discussed in Section 8.

Let a constant oblique force $\mathbf{F} = (E\cos\beta, -E\sin\beta)$ act in the half-plane $y \geqslant L/2$ above the box, and a symmetric force $\mathbf{F} = (-E\cos\beta, E\sin\beta)$ act below the below the box, in the area $y \leqslant -L/2$. Here $0 < \beta < \pi/2$ is a fixed parameter and $E > 0$ is very large, "almost infinite." Such a force effectively replaces the walls. The force is accompanied by a

Gaussian constraint which keeps the kinetic energy of the particle fixed.[7,8] The motion of a single particle in the region $y \geqslant L/2$ is then governed by the equations

$$\dot{x} = v_x, \qquad \dot{y} = v_y$$

and $\dot{\mathbf{v}} = \mathscr{F}_{ts}$ is given by

$$\dot{v}_x = E\cos\beta - \alpha v_x$$

$$\dot{v}_y = -E\sin\beta - \alpha v_y$$

where

$$\alpha = \frac{Ev_x\cos\beta - Ev_y\sin\beta}{v_x^2 + v_y^2} \tag{A.1}$$

so that v^2 is constant. Symmetric equations hold for $y \leqslant -L/2$.

Taking now the limit $E \to \infty$, we find that this model reduces to our Maxwell-demon model (2.1) with a specific function $f = f_\beta$. To obtain that, we take advantage of the conservation of kinetic energy and rewrite the system (A.1) as

$$\begin{aligned} \dot{x} &= v\cos\theta \\ \dot{y} &= v\sin\theta \\ \dot{\theta} &= -\frac{E}{v}\sin(\theta+\beta) \end{aligned} \tag{A.2}$$

where $\theta = \tan^{-1}(v_y/v_x)$ is the angle between the velocity vector (v_x, v_y) and the x axis. The last equation in (A.2) is independent of the first two, and has an implicit solution given by

$$\ln\left[\frac{1+\cos(\theta+\beta)}{1-\cos(\theta+\beta)}\right] = 2\frac{Et}{v} \tag{A.3}$$

It is, however, more convenient to differentiate θ with respect to the height $h = y - L/2$, yielding

$$\frac{d\theta}{dh} = -\frac{E}{v^2}\frac{\sin(\theta+\beta)}{\sin\theta} \tag{A.4}$$

An implicit solution of this equation is

$$(\theta+\beta)\cos\beta-\sin\beta\cdot\ln|\sin(\theta+\beta)|=-\frac{Eh}{v^2} \tag{A.5}$$

Since $h=0$ both as the particle enters the force zone and as it leaves it, the relation between the incoming angle $\varphi=\theta_{\text{in}}$ and the outgoing angle $\psi=-\theta_{\text{out}}$ is determined by the equation

$$F_\beta(-\psi)=F_\beta(\varphi) \tag{A.6}$$

where

$$F_\beta(\theta):=(\theta+\beta)\cos\beta-\sin\beta\cdot\ln|\sin(\theta+\beta)| \tag{A.7}$$

These equations do not contain the force strength E. By taking the limit $E\to\infty$ we simply assure that the particle leaves the force zone instantly, the moment it enters it. Therefore, the infinite force acts like a well at which the particle gets reflected, and the outgoing angle ψ is related to the incoming angle φ by Eq. (2.1) with $f_\beta(\varphi)=-F_\beta^{-1}F_\beta(\varphi)$.

For E very large the time any particle spends in the foce zone is extremely short, so we can neglect possible collisions between particles while one of them is in that zone. In fact if a particle enters the foce zone at time s and leaves it at time $s+\tau$, we can assume that there is no other particle in the force zone between s and $s+\tau$. Under these conditions the analysis of Section 8 takes on a particularly simple form.

Assuming that the stationary state is one of LTE, the one-particle distribution *in the region of the field* is a local Maxwellian where $\Psi(\mathbf{r},\mathbf{v})$ is given by

$$\Psi(\mathbf{r},\mathbf{v})=n(\mathbf{r})(2\pi T_w)^{-1}\exp\{-(\mathbf{v}-\mathbf{v}_w)^2/2T_w\} \tag{A.8}$$

Using the definition of $\bar{M}_l$ in (8.23) with $\mathscr{F}_{\text{ts}}$ given in (A.1), we obtain

$$\begin{aligned}\bar{M}_l&=-\int d\mathbf{r}\int\left(\frac{\partial}{\partial\mathbf{v}}\mathscr{F}_{\text{ts}}\right)\Psi(\mathbf{r},\mathbf{v})\,d\mathbf{v}\\&=-\int d\mathbf{r}\int\frac{(\mathbf{v}-\mathbf{v}_w)}{T_w}\mathscr{F}_{\text{ts}}\Psi(\mathbf{r},\mathbf{v})\,d\mathbf{v}\\&=\frac{\mathbf{v}_w}{T_w}\int d\mathbf{r}\int\dot{\mathbf{v}}\Psi(\mathbf{r},\mathbf{v})\,d\mathbf{v}\end{aligned} \tag{A.9}$$

In going from the second to the third equality on the right side of (A.9) we used the conservation of energy by $\mathscr{F}_{ts}$, i.e., $\dot{\mathbf{v}} \cdot \mathscr{F}_{ts} = 0$. The final term is easily recognized as corresponding to the last term in (8.4), giving the entropy production due to $\mathscr{F}_{ts}$. It becomes equal to $\bar{R}_l$ in (4.2) in the limit $E \to \infty$, giving $\bar{M}_l = \bar{R}_l$ for such systems in LTE.

ACKNOWLEDGMENTS

During the course of this work we have benefited from discussions with many colleagues. In particular, we thank F. Alexander, H. van Beijeren, F. Bonetto, E. Carlen, O. Costin, J. Erpenbeck, G. Eyink, G. Gallavotti, S. Goldstein, W. Hoover, J. Koplik, Ya. Sinai, H. Spohn, and H. T. Yau for various helpful suggestions. We also received a preprint by Ch. Dellago and H. A. Posch,[37] who compute the Lyapunov exponents for our b and c models. Research was supported in part by AFOSR grant AF-92-J-0115, NSF grants DMR 92-13424 and DMS-9401417, and a Faculty Research Grant at the University of Alabama at Birmingham.

REFERENCES

1. L. D. Landau and E. M. Lifshitz, *Fluid Mechanics*, 2nd ed. (Pergamon Press, Oxford, 1987); D. F. Rogers, *Laminar Flow Analysis* (Cambridge University Press, Cambridge, 1992); S. R. de Groot and P. Mazur, *Non-Equilibrium Thermodynamics* (North-Holland, Amsterdam, 1962); R. Balian, *From Microscopies to Macroscopics* (Springer-Verlag, Berlin, 1991), esp. Chapter 14.
2. M. Gross and P. C. Hohenberg, *Rev. Mod. Phys.* **65**:851 (1993).
3. M. Q. Zhang, J.-S. Wang, J. L. Lebowitz, and J. L. Vallés, *J. Stat. Phys.* **52**:1461 (1988); J. R. Dorfman, T. R. Kirkpatrick, and J. V. Sengers, Long range correlations in molecular fluids, *Annu. Rev. Phys. Chem.* **45**:213 (1994).
4. J. L. Lebowitz and P. G. Bergmann, Irreversible Gibbsian ensembles, *Ann. Phys.* **1**:1 (1957); S. Goldstein, N. I. Ianiro, and C. Kipnis, *J. Stat. Phys.* **41**:915 (1985).
5. S. Goldstein, J. L. Lebowitz, and K. Ravishankar, Approach to equilibrium in models of a system in contact with a heat bath, *J. Stat. Phys.* **43**:303 (1986); J. L. Lebowitz and H. Spohn, Stationary non-equilibrium states of infinite harmonic systems, *Commun. Math. Phys.* **54**:97 (1977).
6. H. A. Posch and W. G. Hoover, *Phys. Rev. A* **39**:2175 (1989); W. G. Hoover, H. A. Posch, and C. G. Hoover, *Chaos* **2**:245 (1992); H. A. Posch and W. G. Hoover, in *Molecular Liquids: New Perspectives in Physical Chemistry*, J. J. C. Teixeira-Dias, ed. (Kluwer, Dordrecht, 1992).
7. D. Evans and G. Morriss, *Statistical Mechanics of Nonequilibrium Liquids* (Academic Press, New York, 1990).
8. W. G. Hoover, *Computational Statistical Mechanics* (Elsevier, Amsterdam, 1991).
9. N. I. Chernov, G. L. Eyink, J. L. Lebowitz, and Ya. G. Sinai, *Phys. Rev. Lett.* **70**:2209 (1993); *Commun. Math. Phys.* **154**:569 (1993).

10. G. L. Eyink and J. L. Lebowitz, Generalized Gaussian dynamics, phase-space reduction, and irreversibility: A comment, in *Microscopic Simulations of Complex Hydrodynamic Phenomena*, M. Mareschal and B. L. Holian, eds. (Plenum Press, New York, 1992), p. 323; G. Gallavotti, Ergodicity, ensembles, irreversibility in Boltzmann and beyond, *J. Stat. Phys.* **78**:1571–1589 (1995).
11. H. Spohn, *Large Scale Dynamics of Interacting Particles* (Springer-Verlag, Berlin, 1991); A DeMasi and E. Presutti, *Mathematical Methods for Hydrodynamic Limits* (Springer-Verlag, Berlin, 1991); J. J. Lebowitz, E. Presutti, and H. Spohn, Microscopic models of hydrodynamical behavior, *J. Stat. Phys.* **51**:841–862 (1988); G. Eyink, J. L. Lebowitz, and H. Spohn, *Commun. Math. Phys.* **140**:119 (1991).
12. W. G. Hoover, H. A. Posch, B. L. Holian, M. J. Gillan, M. Mareschal, and C. Massobrio, *Mol. Simul.* **1**:79 (1987); D. J. Evans, E. G. D. Cohen, and G. P. Morriss, *Phys. Rev. A* **42**:5990 (1990); see also J. R. Dorfman, From molecular chaos to dynamical chaos, Lecture Notes, preprint (1995).
13. D. J. Evans, E. G. D. Cohen, and G. P. Morriss, Probability of second law violations in shearing steady flows, *Phys. Rev. Lett.* **71**:2401–2404 (1993).
14. G. P. Dettman and G. P. Morriss, Proof of conjugate pairing for an isokinetic thermostat, preprint (1995).
15. G. Gallavotti and E. G. D. Cohen, Dynamical ensembles in stationary states, *J. Stat. Phys.* **80**:931–970 (1995).
16. G. Gallavotti, In *Topics in Chaotic Dynamics*, P. L. Garrido and J. Marro, eds. (Springer-Verlag, Berlin, 1995); G. Gallavotti, Reversible Asonov diffeomorphisms and large deviations, *Math. Phys. Electron. J.* **1**:1–12 (1995); G. Gallavotti, Chaotic hypothesis: Onsager reciprocity and fluctuation-dissipation theorem, *J. Stat. Phys.* **84**:899–925.
17. F. Bonetto and G. Gallavotti, Reversibility, coarse graining and the chaoticity principle, preprint (1996).
18. F. Bonetto, N. Chernov, and J. L. Lebowitz, In preparation.
19. W. T. Ashurst and W. G. Hoover, *Phys. Rev. A* **11**:658 (1975); J. Koplik, J. R. Banavar, and J. F. Willemson, *Phys. Rev. Lett.* **60**:1282 (1988); L. Hannon, G. C. Lie, and E. Clementi, *J. Stat. Phys.* **51**:965 (1988); D. Rapaport, *Phys. Rev. Lett.* **60**:2480 (1988); *Phys. Fluids A* **1**:781 (1989); *Phys. Rev. A* **46**:1971 (1992); *Transport Theory Stat. Phys.* **23**:235 (1994).
20. N. Chernov and J. L. Lebowitz, Stationary shear flow in boundary driven Hamiltonian systems, *Phys. Rev. Lett.* **75**:2831–2834 (1995).
21. L.-S. Young, Dimension, entropy and Lyapunov exponents, *Ergod. Theory Dynam. Syst.* **2**:109–124 (1982).
22. Ya. B. Pesin, On rigorous mathematical definitions of correlation dimension and generalized spectrum for dimensions, *J. Stat. Phys.* **71**:529–547 (1993).
23. D. Ruelle, Positivity of entropy production in nonequilibrium statistical mechanics, *J. Stat. Phys.*, to appear (October 1996); see also G. Gentile, Large deviation rule for Anosov flows, IHES preprint (1996).
24. R. Esposito, J. L. Lebowitz, and R. Marra, Hydrodynamic limit of the stationary Boltzmann equation in a slab, *Commun. Math. Phys.* **160**:49 (1994).
25. J. L. Lebowitz, *Physica A* **194**:1 (1993); Boltzmann's entropy and time's arrow, *Phys. Today* **46**:32–38; **47**:113–116 (1993); Microscopic reversibility and macroscopic behavior: Physical explanations and mathematical derivations, in *25 Years of Non-Equilibrium Statistical Mechanics*, J. J. Brey, J. Marro, J. M. Rubi, and M. San Miguel, eds. (Springer, New York, 1995).
26. F. Alexander, Private communication.
27. C. Cercignani, *Mathematical Methods in Kinetic Theory* (Plenum Press, New York, 1990).

28. G. Gallavotti and P. Garrido, Billiards correlation functions, *J. Stat. Phys.* **76**:549–585 (1994); O. E. Lanford, Some informal remarks on the orbit structure of discrete approximations to chaotic maps, preprint, ETH, Zurich (1996).
29. R. Bowen, *Equilibrium States and the Ergodic Theory of Anosov Diffeomorphisms* (Springer-Verlag, Berlin, 1975).
30. T. Krüger and S. Troubetzkoy, Markov partitions and shadowing for nonuniformly hyperbolic systems with singularities, *Ergod. Theory Dynam. Syst.* **12**:487–508 (1992).
31. D. Gass, Enskog theory for a rigid disk fluid, *J. Chem. Phys.* **54**:1898–1902 (1971); D. Risso and P. Cordero, *J. Stat. Phys.* **82**:1453–1466 (1996).
32. J. Erpenbeck and W. Wood, Molecular-dynamics calculations of the velocity autocorrelation function. Methods, hard disk results, *Phys. Rev. A* **26**:1648–1675 (1982).
33. F. Ree and W. Hoover, Fifth and sixth virial coefficients for hard spheres and hard disks, *J. Chem. Phys.* **40**:939–950 (1964); E. Helfand, H. Frisch, and J. L. Lebowitz, Theory of two- and one-dimensional rigid sphere fluids, *J. Chem. Phys.* **34**:1037 (1960).
34. S. Olla, S. R. S. Varadhan, and H. T. Yau, Hydrodynamic limit for a Hamiltonian system with weak noise, *Commun. Math. Phys.* **155**:523–560 (1993); Y. G. Sinai, *Selecta Math. Sov.* **7**:279 (1988).
35. D. N. Zubarev, *Nonequilibrium Statistical Thermodynamics* (Consultants Bureau, New York, 1974); J. A. McLennan, *Introduction to Nonequilibrium Statistical Mechanics* (Prentice-Hall, Englewood Cliffs, New Jersey, 1989); G. L. Eyink, J. L. Lebowitz, and H. Spohn, Hydrodynamics and fluctuations outside of local equilibrium: Driven diffusive systems, *J. Stat. Phys.* **83**:385–472 (1996).
36. I. Newton, *The Mathematical Principles of Natural Philisophy*, Book II, Section VIII, Proposition XLVIII, Theorem XXXVIII, p. 305.
37. R. Lupton, *Statistics in Theory and Practice* (Princeton University Press, Princeton, New Jersey, 1993).
38. Ch. Dellago and H. A. Posch, Lyapunov instability of the boundary driven Chernov–Lebowitz model for stationary shear flow, University of Vienna, preprint (May 1996).